Third International Conference on Sustainable Construction Materials and Technologies http://www.claisse.info/Proceedings.htm

Changes in Pore Structure by a Silicate-based Surface Penetrant and Their Effects on Mechanical and Transport Properties in Cement Pastes

Shingo Watanabe[1] and Shin-ichi Igarashi[1]

[1]*Kanazawa University, Japan*
n0311@yahoo.co.jp, igarashi@se.kanazawa-u.ac.jp

ABSTRACT

Microstructure in cement paste impregnated with a silicate-based surface penetrant was examined by SEM/BSE image analysis. Improvements of mechanical properties and permeability by the surface treatment were evaluated by microhardness testing and measurement of electrical conductivity. Increase in the surface hardness was related to characteristic changes in capillary pore structure revealed by the image analysis. The degree of hydration of cement increased a little with time in the treated region. Coarse capillary pore structure did not appreciably change by the treatment. Nevertheless, the hardness in the treated region increased with time. This fact suggests that the penetrant decreased porosity of fine pores smaller than the resolution of the BSE image. The decrease in the fine porosity was calculated by combining the Powers model and an empirical relationship between microhardness and compressive strength for cement pastes. The calculated fractions of the pore phases were consistent with the results of image analysis.

Keywords. silicate-based surface penetrant, porosity, image analysis, microhardness, Powers' model

INTRODUCTION

In order to improve mechanical properties and to provide resistivity against ingress of harmful substances, several methods to enhance surface properties of concrete have been developed. Of them, impregnation of silicate-based surface penetrants is increasingly being applied to concrete structures. This treatment forms dense surface regions due to reaction of the penetrant with calcium hydroxide in concrete. Taking account of its usefulness for prolonging life of concrete, this method is a promising way to obtain sustainable concrete structures.

However, on the other hand, the depth of penetration is relatively small. The treated region does not change its original colour even though substantial penetration is attained. Therefore, it is not easy to determine an exact depth to which a penetrant modifies microstructure. Furthermore, commercial products of the penetrants usually contain some other components or ingredients to have additional functions. Therefore, effects of silicate-based penetrants themselves on the evolution of microstructure have not been fully understood.

In this study, capillary pore structure in a cement paste impregnated with a silicate-based surface penetrant was examined by a SEM/BSE image analysis technique. Improvement in mechanical properties was evaluated by microhardness testing. Effects of the surface treatment on transport properties were also evaluated by measurement of electrical conductivity. Changes in those physical properties were discussed in relation to characteristics in the capillary pore structure.

EXPERIMENTAL

Materials and production of cement paste specimens. The cement used was ordinary Portland cement. The penetrant used was a commercial product of which main components were sodium and potassium silicates. Its properties are given in Table 1.

Table 1 Properties of a penetrant

Appearance	colourless, inodorous
Density (g/cc)	≥1.3 (concentrated liquid)
pH	≥11
Content of main components	≥30% ($X_2SiO_2 \cdot nH_2O$)
Amount of coating	0.24kg/m^2 (diluted with water; 1:1solution)

Cylindrical specimens of 200mm in height and 100mm in diameter were produced in accordance with JIS R5201. The water/cement ratio was 0.50. They were demolded at 24h after casting, and then cured in water at 20ºC. At the age of 7days, disk specimens of 50mm and 25mm in thickness were cut from the middle in the specimens. The disk specimens were then cured in the moist condition of 80%R.H. for 7days. After the moist curing, surfaces of the disk specimens were coated with the silicate-based surface penetrant. Then, they were cured again in the moist room so that reaction of the silicate-based penetrant properly took place. Disk specimens of cement paste without any treatment were also produced. They were continuously cured in water after demolding. These specimens of continuous water curing are used as the controls in this study.

Microhardness testing. At 14, 28 and 77days after coating (i.e. the ages of specimens were 28, 42 and 91days, respectively), small cubes of 20mm edge length were taken from the surface regions, which had been coated with the penetrant. A cross section of the small cube was carefully polished with SiC papers. Microhardness (Vickers) was obtained in the polished section. The load of indentation was 0.098N.

Electrical conductivity. The disk specimens of 100mm in diameter and 50mm in height were used. Electrical conductivity was measured using equipment used in ASTM C1202 (Fig. 1) (Nokken and Hooton, 2006). The applied voltage (V) was 30V. The both cells were filled with 0.3N sodium hydroxide solution. The current (I) was measured at 15 minutes after applying the voltage. Bulk conductivity (σ) was calculated using the following formula:

$$\sigma = \frac{I \cdot L}{V \cdot A} \quad (1)$$

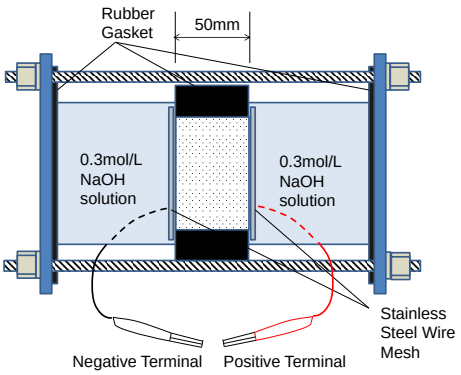

Fig. 1 Testing apparatus for conductivity

where A and L are the cross-sectional area and the thickness of the specimen, respectively.

Image analysis. At the ages of 28, 42 and 91days, slices about 10 mm in thickness were cut from the cylinder specimens. They were dried by ethanol replacement and subsequently by freeze drying procedure with t-butyl alcohol. Then, they were impregnated with a low viscosity epoxy resin. After the resin hardened at room temperature, the slices were finely polished with SiC papers. The polished surfaces were finished with a diamond slurry for a short time.

Samples were examined using an SEM equipped with a quadruple backscatter detector. The backscattered electron (BSE) images were acquired at a magnification factor of 500x. Each BSE image consists of 1148×1000 pixels. The size of one pixel is about 0.22 μm×0.22 μm. Pixels for residual unhydrated cement particles and for pores were counted in order to obtain the area fractions of these two phases. Using the Delesse principle in stereology (Mouton, 2002), the area fractions of a phase in 2-D cross sections are assumed to be equal to its 3-D volume fractions. The degree of hydration of cement (α) was calculated with the following equation;

$$\alpha = 1 - \frac{UH_i}{UH_0} \tag{2}$$

where UH_i is an area fraction of unhydrated cement particles at the age of t_i, and UH_0 is the initial area fraction of unhydrated cement particles, which is determined by the mix proportion. The pore pixels tallied in the images form agglomerations. Each pore cluster was converted to the equivalent circle, which had the same area as the original cluster. Pore size distribution curves for the pores were obtained by arranging those equivalent circles in order (Diamond and Leeman, 1995).

Furthermore, using the degree of hydration and the Powers model for the hydration of cement (Powers, 1949), the volume fractions of cement gel were calculated. Then, the total capillary porosity was obtained by subtracting the sum of volumes of the unhydrated cement and the cement gel from the total volume of cement paste. The difference between the calculated total porosity and the porosity directly evaluated by the image analysis was considered as fine porosity, of which sizes were smaller than the resolution. This procedure was applied to the treated region and the bulk cement paste of the control (Igarashi et al. 2005).

Spatial structure of pores. It seems that not only the porosity but also spatial structure of pores affects properties of cement paste, in particular transport properties through the body. To evaluate the spatial structure, the nearest neighbourhood distance function was obtained for the pores in BSE images. At first, the pore clusters in BSE images were converted to points, of which locations were coincident with gravity centres of each cluster. The resultant points dispersed in a observation window were considered as a point process $X=\{\boldsymbol{x}_i : \boldsymbol{x}_i \in W\}$(Stoyan, et al. 1995) . Hanisch's nearest neighbour distance function $\widehat{G}(r)$ (Hanisch, 1984) for the point process was calculated using Eq. (3).

$$\hat{G}(r) = \frac{\sum_{i=1}^{N(W)} \mathbf{1}(s_i \le r) \cdot \mathbf{1}(s_i \le b_i) \cdot w(s_i)}{\sum_{i=1}^{N(W)} \mathbf{1}(s_i \le b_i)\, w(s_i)} \tag{3}$$

where $1(\cdot)$ is the indicator function, i.e. equal to one if its argument is true and zero otherwise. N(W) is the number of points in the observation window $W = x \times y$, and b_i is the

shortest distance from each point $\boldsymbol{x}_i$ to edges of the window. s_i is the distance to the nearest point of the point process. $w(s_i)$ is a weighting factor, and given as the inverse of the window area eroded by a circle of radius s_i (Eq.(4)).

$$w(s_i) = \{(x - 2s_i)(y - 2s_i)\}^{-1} \quad (4)$$

RESULTS

Improvements in properties of cement paste. SEM micrographs for cement pastes with and without the penetrant are shown in Fig. 2. It seems that there are no distinct differences in appearance between the treated surface region and the bulk cement paste cured in water. Even in the treated cement paste (Fig.2(a)), there remained many coarse pores. Microhardness distributions in surface regions of the cement pastes treated with the penetrant are shown in Fig.3. The broken horizontal lines are the microhardness obtained for the cement pastes continuously cured in water. The microhardness in the treated surface regions was greater than in the inner part of the cement paste. It decreased with distance from the surface. The depth at which the microhardness was almost comparable to that of the cement paste cured in water increased with time. However, the depths of greater microhardness were not so great on the whole. The dense region due to reaction of the penetrant extended at most to 10mm or less even at the long age of 91days. Electrical conductivities of cement pastes are shown in Fig. 4. The conductivity of the treated specimen at 28days was lower than that of the control specimen. This means that the surface treatment resulted in dense and disconnected networks of capillary pores. However, there are no

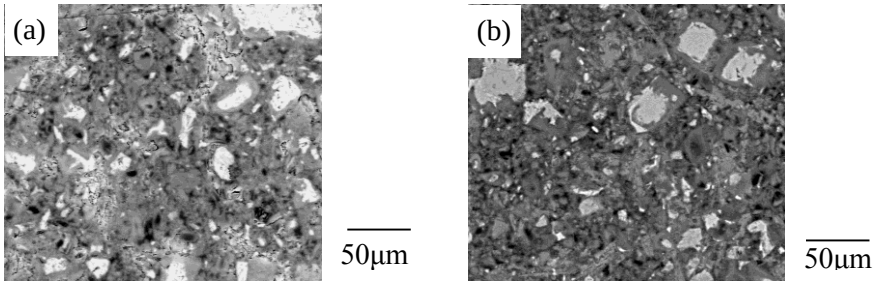

Fig.2 BSE images of cement pastes: (a) surface region treated with the penetrant (b) bulk cement paste cured in water

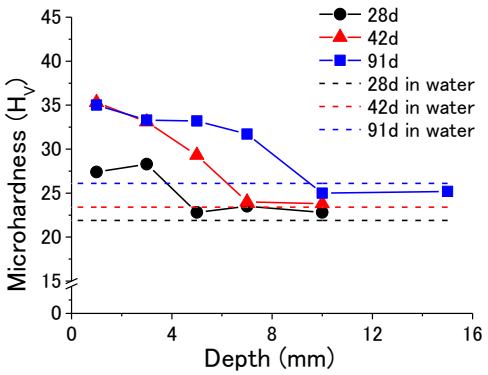

Fig. 3 Changes in microhardness with the depth from the surface

differences in the conductivity between the treated specimens and the control ones at longer ages. It is clearly found from Figs. 3 and 4 that mechanical and transport properties of cement paste, at least in the surface regions were enhanced by the treatment.

Fig. 5 shows degrees of hydration of cement at surface regions. The broken lines in Fig. 5 indicate the degrees of hydration of cement in the bulk cement pastes that were continuously cured in water. The degrees in the treated regions were always smaller than those in the controls. Furthermore, the degrees at the depth of 1mm are slightly smaller than those at 10mm. In other words, the hydration of cement did not proceed well in the treated surface region even when the specimens were cured in the moist condition, which was recommended for the penetrant. Nevertheless, mechanical and transport properties were appreciably improved, as shown in Figs. 3 and 4. This fact also suggests that dense microstructure in the surface regions was contributed from not only the hydration of cement but also a reaction of the silicate-based penetrant, and that the latter significantly affected the physical properties mentioned above.

DISCUSSION

Characteristics in pore structure. Volume fractions of constituent phases in cement

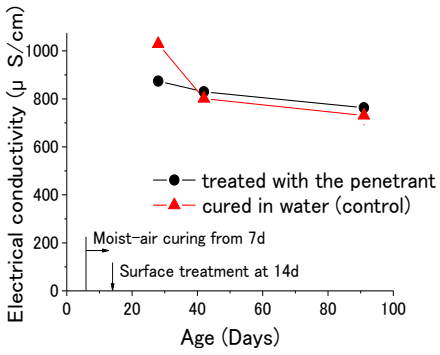

Fig.4 Comparison of bulk conductivity between treated and control specimens

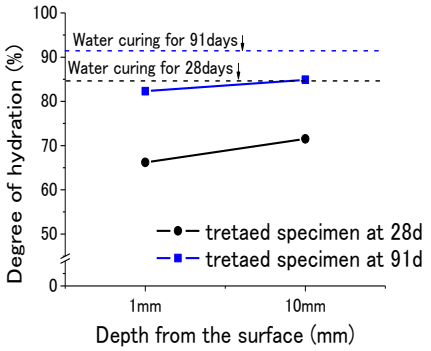

Fig.5 Degrees of hydration of cement at the surface regions

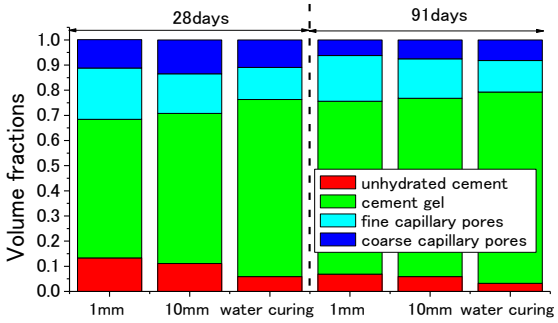

Fig.6 Comparison of volume fractions of constituent phases between the treated and the control specimens

pastes are shown in Fig. 6. These fractions are calculated using the degrees of hydration (Fig. 5) and the Powers model. Regardless of ages and depths from the surface, the fractions of solid phases in the treated regions are smaller than those in the controls cured in water. Coarse capillary porosity in the treated regions was not always smaller than in the control at 28 days. These volume fractions imply the treated regions are more porous than the controls. However, this clearly contradicts the results of greater microhardness and lower electrical conductivities in the treated specimens (Figs.3 and 4). Therefore, the calculated volume fractions in Fig. 6 must be modified. Taking into account the fact that the volumes of unhydrated cement and the coarse capillary porosity are directly evaluated from the BSE images, and that the volume of cement gel is determined by a reliable hydration model of Powers, the amounts of fine capillary pores should be modified. Actually, in the calculation for Fig. 6, only a phase of fine capillary porosity is indirectly evaluated by subtracting those known volumes from the total volume of cement paste. If such a modification to the calculated volume fractions is made, it is suggested that reaction of the silicate-based penetrant more effectively reduces fine capillary pores of which diameters are smaller than the resolution of 0.2μm in this study.

Fig. 7 shows pore size distribution curves for coarse capillary pores. The treated regions contain more large pores of which diameters are larger than 10μm. The amount of such a large pore is quite little in the controls. Therefore, the pore structure in the treated region seems more porous than the control. However, on the other hand, the controls contain considerable amounts of pores smaller than 2μm at 28days whereas the surface region in the treated specimen has little. This tendency to decrease fine pores in the treated region is more

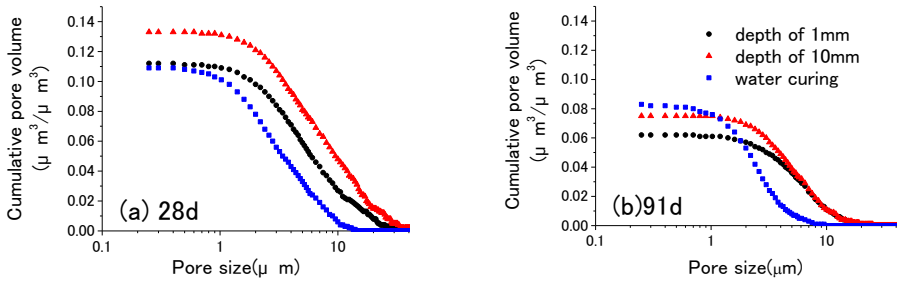

Fig. 7 Pore size distribution for coarse capillary pores

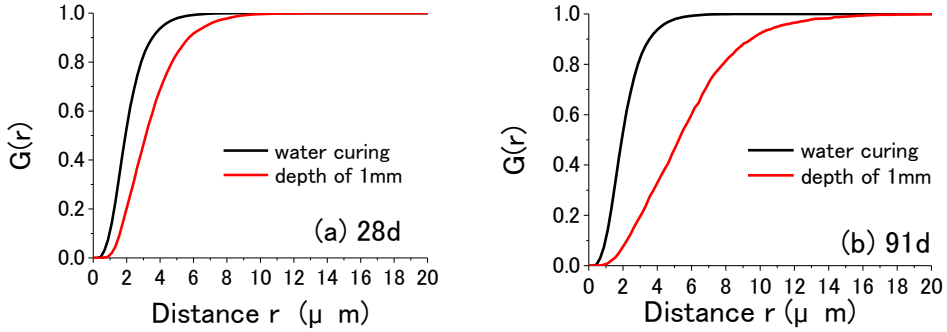

Fig. 8 Nearest-neighbour distance function for coarse capillary pores

remarkable at 91days. At the depths of 1 and 10mm, there are no pores smaller than 2-3μm in the treated regions. Furthermore, it should be noted that the coarse capillary porosity itself in the treated region is smaller than in the control at 91days. Namely, the penetrant changes pore size distribution in the range of coarse pores. These changes in coarse capillary pore structure also suggest that smaller pores are preferably filled with reaction products of the penetrant, as mentioned previously.

Fig. 8 shows comparison of the nearest-neighbour distance functions for coarse capillary pores between the treated region and the control. Distances at which the function converges to the unity are two or three times greater in the treated region than in the control. All the pores in an observation window are represented by points in this statistical approach. Therefore, the longer distance of convergence means some capillary pores are deleted so that distances between points are increased. This deletion of pores seems to be reflected to the increase in the surface microhardness, as shown in Fig. 3. When hydration of cement takes place normally as in the control specimen, the total porosity, the maximum diameter and also the threshold diameter are gradually decreased. The resultant pore structure is a pore network where pore size distribution is continuous. In other words, the pore structure contains pores of any ranges of pore sizes. In contrast to the process of hydration of cement, the reaction of the penetrant seemed to decrease specific ranges of pore sizes while the greater pores still remained at long ages. This change in pore structure resulted in a discontinuous pore network such that the path of electrical conductivity could be effectively closed.

Interpretation of increase in surface hardness as an increase in solid volume. As found from Fig. 4, the depth of enhancement by the penetrant is at most a few mm.

Table 2 Compressive strength estimated from microhardness

	28days			42days		91days		
Depth	1mm	10mm	Water curing	1mm	10mm	1mm	10mm	Water curing
Hv	27.4	22.8	21.9	35.3	23.8	35.0	24.7	26.1
f'_c(N/mm^2)	39.8	33.2	31.8	51.3	34.5	50.9	35.9	37.9

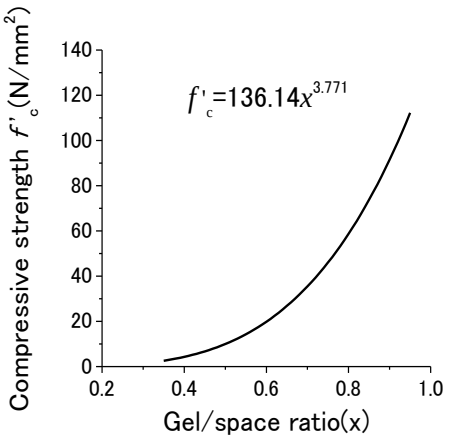

Fig. 9 Compressive strength vs. gel/space ratio for hardened cement pastes

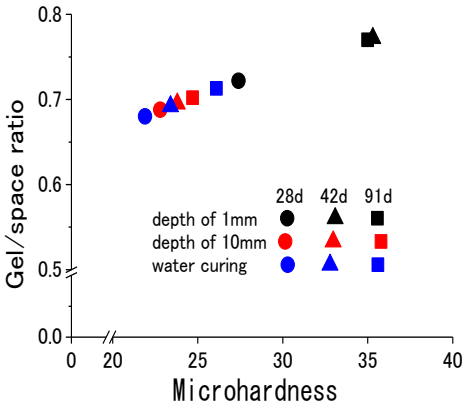

Fig. 10 Relationship between gel/space ratio and microhardness

Therefore, it is difficult to understand an increase in surface hardness as a common sense of strength. Taking account of practical applications and objectives of the penetrant in situ, it is useful to intuitively understand the increase in hardness as an enhancement of compressive strength. Feldman and Huang (1985) have proposed a linear relationship between microhardness and compressive strength in cement pastes. Using their results, compressive strength of cement pastes is simply related to microhardness, as follows;

$$H_V = 0.688 f'_c \tag{5}$$

where H_V is Vickers microhardness, and f'_c is compressive strength of cement paste. Substituting the measured values of microhardness into Eq.(5), the corresponding local compressive strength for the cement paste is estimated, as shown in Table 2. Treatment with the penetrant resulted in about 7-10N/mm^2 increase in compressive strength at the surface region whereas the degree of hydration of cement was smaller in that region (Fig. 3). Once the compressive strength is determined, the corresponding gel/space ratio in the Powers model is also calculated. Using the compressive strength vs. the gel/space ratio relationship proposed by Watanabe (2005) (Fig. 9), a relationship between the estimated gel/space ratios and measured values of microhardness is obtained, as shown in Fig. 10. Regardless of curing conditions and the surface treatment, there exists a liner relationship between the gel/space ratio and the microhardness.

Then, once the gel/space ratios for the treated regions are known, volume fractions of constituent phases in the treated region are calculated as well as in the control of which volume fractions are determined by the degree of hydration of cement. In other words, modified volume fractions corresponding to the increase in microhardness are obtained for the treated region. A comparison of the calculated volume fractions is shown in Fig. 11. The volume fraction based simply on the degree of hydration is shown in Fig. 11 (a) and (c). In the calculation of modified fractions in Fig. 11 (b) and (d), changes in the gel/space ratio due to the reaction of the penetrant are taken into account in addition to the hydration of cement.

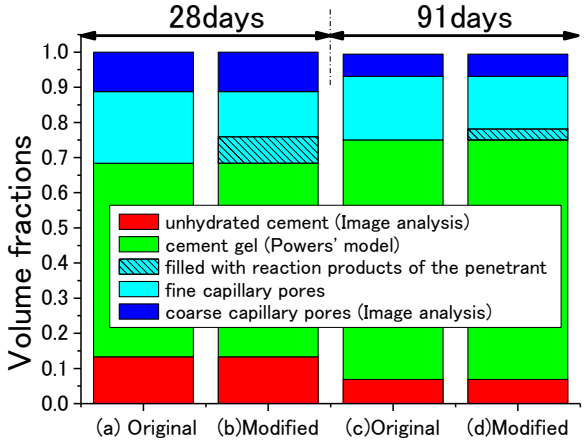

Fig. 11 Modification of volume fractions of fine capillary porosity at the depth of 1mm; (a) Original fractions based only on the degree of hydration at 28d (b) Fractions modified to adjust to the increase in microhardness at 28d (c) Original fractions based only on the degree of hydration at 91d (d) Fractions modified to adjust to the increase in microhardness at 91d

Substantial parts of fine pores in the original porosity were replaced with the reaction product of the penetrant at 28days. It should be noted that the decreases in the fine porosity does not contradict the volume changes in the Powers model and also the experimental results of image analysis. In other words, an increase in microhardness is consistent with the inference above that fine capillary porosity was preferably reduced by the treatment with the silicate-based penetrant.

CONCLUSIONS

Microstructure in cement pastes treated with a silicate-based penetrant was examined by SEM-BSE image analysis. Changes in surface physical properties of the cement pastes were related to characteristics of the microstructure revealed by the image analysis. Major outcomes are as follows;

(1) Surface microhardness of cement paste was increased by the application of the silicate-based penetrant. However, the depth of region with greater microhardness extended at most 10mm at long ages.

(2) Degrees of hydration of cement in the treated region were not so high compared to those in the specimens cured in water. Nevertheless, the electrical conductivity of the treated specimen was almost comparable to the controls.

(3) The surface penetrant effectively decreased fine capillary porosity while large pores were still remained at long ages. Then, such a filling process for pores may result in a gap-graded pore structure. This led to the decrease in the electrical conductivity.

(4) A way to interpret the increase in surface microhardness as a change in volume fractions of constituent phases was proposed using an empirical relationship between microhardness and compressive strength. The estimated volume fractions were consistent with the Powers model and the results of the image analysis.

(5) The estimated fraction also suggests that the penetrant effectively reduces fine capillary porosity which is less than the resolution of the image analysis.

ACKNOWLEDGEMENT

The authors acknowledge financial support from the Japan Society for the Promotion of Science (JSPS) through Grant-in-Aid for Scientific Research (A) (No.23246081, Project manager : K. Takewaka (Kagoshima University)) and (C) (No.21560482).

REFERENCES

Diamond, S. and Leeman, M.(1995). “Pore size distribution in hardened cements pastes by SEM image analysis.” Microstructure of cement-based system/Bonding and interfaces in cementitious materials, MRS Symp. Proc., Vol.370, pp.217-226.

Feldman, R.F. and Huang, C.Y.(1985).”Properties of Portland cement-silica fume pastes Ⅱ. Mechanical properties.” Cement and Concrete Research, Vol.15, No.6, pp.943-952.

Hanisch, K.H. (1984). “Some remarks on estimators of the distribution function of nearest neighbour distance in stationary spatial point patterns,” Math. Oberforsch. Statist. Ser. Statist. Vol.15, pp.409-412.

Igarashi, S., Watanabe, A. and Kawamura, M.(2005).”Evaluation of capillary pore size characteristics in high-strength concrete at early ages,” Cement and Concrete Research, Vol.35, No.3, pp.516-519.

Mouton, P.R. (2002) “Principles and practices of unbiased stereology, An introduction for bioscientists.” The Johns Hopkins University Press, Baltimore and London.

Nokken, M.R. and Hooton, R.D. (2008). “Using pore parameters to estimate permeability or conductivity of concrete.” Materials and Structures, Vol.41, No.1, pp.1-16.

Powers, T.C.(1949).”The non-evaporable water content of hardened Portland cement paste.” ASTM Bulletin,” No.158, pp.68-76.

Stoyan, D., Kendall, W.S. and Mecke, J.(1995). “Stochastic geometry and its application,” second edition, John Wiley and Sons, Chichester, England.

Watanabe, A.(2005). “Study on quantitative evaluation of microstructure in cement paste by SEM-BSE image analysis technique.” Doctor thesis, Kanazawa University.